Remote Sensing of Environment 347 (2026) 115648

Contents lists available at ScienceDirect

Remote Sensing of Environment

journal homepage: www.elsevier.com/locate/rse

The intercomparison of total column water vapor over a melting glacier on the Greenland ice sheet derived using spaceborne Sentinel-5P and high spatial resolution EnMAP measurements

Alexander Kokhanovsky [a,*], Luca Lelli [b], Karl Segl [c], Jörg Bendix [a]

[a] Climatology and Remote Sensing Laboratory at the Department of Geography of Philipps Marburg University, Marburg, Germany
[b] Remote Sensing Institute at the German Aerospace Center (DLR), Wessling, Germany
[c] Helmholtz Centre for Geosciences, Potsdam, Germany

ARTICLE INFO

Edited by Dr. Menghua Wang

Keywords:
Water vapor
Remote sensing
EnMAP
Sentinel-5P
Light absorption
Radiative transfer
Snow
Glacier ice

ABSTRACT

The paper is aimed at the retrieval of total column water vapor (TCWV) over a melting glacier using high spatial resolution hyperspectral measurements performed by the German EnMAP (Environmental Mapping and Analysis Program) satellite. Such measurements are important for understanding the intra-pixel variability of water vapor satellite products with coarser spatial resolution especially in regions with drastic changes in the water vapor abundances. The retrieved TCWV is compared with that derived using other spaceborne optical measurements such as performed by Sentinel-5P. The close correspondence of both retrievals has been found with a smaller variance over derived EnMAP TCWV values.

1. Introduction

Water vapor is one of the main actors in the global hydrological cycle with relevance to climate change studies. This work is aimed at the retrieval of the TCWV over a melting glacier using the Environmental Mapping and Analysis Program (EnMAP) sensor, that provides spectral information from 224 bands in the wavelength range 418–2440 nm with a spatial resolution of 30 m. The advantage of a hyperspectral instrument is not the amount of data in this case, but in the ability to select optimal information in terms of band position and spectral width. Further details on the optical design of the instrument and EnMAP products are given in (Chabrillat et al., 2024; Guanter et al., 2015). We use the approach for the EnMAP TCWV retrieval proposed in (Kokhanovsky et al., 2023a). The technique has been validated using a single ground measurement of water vapor over the snow surface in Antarctica, which is characterized by dry conditions similar to those existing over deserts. In this work we extend the validation procedure comparing the results of the retrieval technique to those derived from Sentinel-5P (S5P) (Chan et al., 2022) over a melting glacier with the values of TCWV much higher as compared to those observed in Antarctica (Kokhanovsky et al., 2023a).

2. The analytical model for the spectral reflectance of underlying glacier ice – atmosphere system

We use the analytical model for the glacier surface – atmosphere spectral reflectance proposed in (Kokhanovsky et al., 2023a; Kokhanovsky et al., 2024; Kokhanovsky, 2022; Kokhanovsky et al., 2026). In particular, the top-of-atmosphere (TOA) reflectance R_{TOA} is modelled as

$$R_{TOA} = \left(R_{atm} + \gamma T_{atm} R_{surf}\right) T_{gas}. \quad (1)$$

Here, R_{atm} is the atmospheric reflectance for the case of a black ground surface, R_{surf} is the ground surface reflectance, T_{gas} is the atmospheric gaseous transmittance term, and T_{atm} is the atmospheric transmittance for the case of a gaseous absorption free atmosphere. The parameter γ accounts for the multiple light scattering between atmosphere and ground surface.

This research was supported by the German Science Foundation (Deutsche Forschungsgemeinschaft, grant no. KO 3671/8–1/AOBJ 712291).

* Corresponding author.
E-mail addresses: akokhanoa@staff.uni-marburg.de (A. Kokhanovsky), luca.lelli@dlr.de (L. Lelli), karl.segl@gfz.de (K. Segl).

https://doi.org/10.1016/j.rse.2026.115648
Received 6 March 2026; Received in revised form 27 July 2026; Accepted 2 September 2026
Available online 4 September 2026
0034-4257/

It has been proposed in (Kokhanovsky et al., 2023a) that the gaseous transmittance can be estimated using Eq. (1):

$$T_{gas} = \frac{R_{TOA,meas}}{R_{TOA,sim}}, \quad (2)$$

where

$$R_{TOA,sim} = R_{atm} + \gamma T_{atm} R_{surf} \quad (3)$$

is the simulated TOA reflectance in the absence of gaseous absorption at the measured channel specified by the wavelength λ. The value of $R_{TOA,sim}$ can be obtained from the solar light reflectance spectrum derived from top-of-atmosphere radiance measurements dividing the spectrum inside the absorption band in two components: one background term slowly changing with the wavelength and another oscillating term due to atmospheric gaseous absorption contribution. Such an approach is often used in the framework of the differential optical absorption spectroscopy (Platt and Stutz, 2026). Quite contrary, in this work we derive the TCWV from the EnMAP measurements at a single wavelength (1128 nm) with significant absorption of light by water vapor and derive the value of $R_{TOA,sim}$ using radiative transfer calculations as proposed in (Kokhanovsky et al., 2023a; Kokhanovsky et al., 2024; Kokhanovsky, 2022; Kokhanovsky et al., 2026). An important point is that TOA reflected solar light intensity measurements at the selected wavelength in the clean polar atmosphere are hardly influenced by atmospheric scattering effects. Therefore, they can be accounted for using the simple radiative transfer approximation as discussed in (Kokhanovsky et al., 2023b). The term R_{surf} in Eq. (3) is modelled as proposed in (Kokhanovsky et al., 2026):

$$R_{surf} = R_0 \exp\left\{-\sqrt{\alpha_{ice} L}\right\}, \quad (4)$$

where R_0 is the surface reflectance for the artificial case of nonabsorbing semi-infinite snow or glacier ice surface, L is the absorption length, α_{ice} is the known bulk ice absorption coefficient. We derive spectrally neutral constants R_0, L from the spectral TOA reflectance as discussed in (Kokhanovsky et al., 2026). Our approach makes it possible to derive the background term slowly varying with the wavelength (see above) directly from radiative transfer calculations avoiding fitting procedures usually applied in the framework of the differential optical absorption spectroscopy. The analytical gaseous transmittance model proposed in the framework of the SNOW and atmosphere reflectance and TRANsmittance radiative transfer model (SNOWTRAN) (Kokhanovsky et al., 2024) has been used to derive the gaseous transmittance T_{gas} in Eq. (2). In the framework of this model it is assumed that

$$T_{gas} = \exp\{-\tau_{WV}\} \quad (5)$$

for the gaseous absorption band located at 1128 nm. Here, τ_{WV} is the effective water vapor total optical thickness modelled as suggested in (Green et al., 1988; Pierluissi and Tsai, 1986; Cachorro et al., 2022):

$$\tau_{WV}(\lambda) = [BMNk(\lambda)]^{\varepsilon}, \quad (6)$$

where

$$B = \left[\frac{P}{P_0}\right]^a \left[\frac{T_0}{T}\right]^b, \quad (7)$$

P and T are average pressure and temperature calculated using respective atmospheric profiles ($P = 800$ hPa and $T = 270$ K for the case studied), $a = 0.781$, $b = 0.439$, P_0 and T_0 are standard pressure and temperature, $\varepsilon = 0.646$, M is the airmass factor, $k(\lambda)$ is the water vapor absorption coefficient and N is the total column of water vapor.

One can see that the inverse problem for the determination of the TCWV can be solved analytically. In particular, it follows:

$$N = \frac{\left[\ln\left[R_{TOA,sim}(\lambda^*)/R_{TOA,meas}(\lambda^*)\right]\right]^{1/\varepsilon}}{BMk(\lambda^*)}, \quad (8)$$

where $\lambda^* = 1128 nm$.

3. Results

In this section we apply the retrieval technique described above for the determination of the total column water vapor over a glacier using EnMAP L1Cdata (at sensor radiance). The EnMAP true color RGB for the area is shown in Fig. 1. The European Centre for Medium-Range Weather Forecasts reanalysis product (ERA5) shows (Hersbach et al., 2020) that temperature was above zero at the studied location/time and, therefore, significant ice and snow melting processes occurred. This has been confirmed by ground observations at the date specified (B. Vandecrux, personal communication).

The result of applying the algorithm to clear sky parts of the glacier surface is given in Fig. 2. The cloud screening and glacier ice pixel selection procedure is described in the Appendix. We have used the geometrical approximation for the airmass factor determined by the cosine of the solar zenith μ and viewing zenith η angles $\left(M = \mu^{-1} + \eta^{-1}\right)$. The values of (P, T) have been estimated using the ERA5 re-analysis data (Hersbach et al., 2020) and it was assumed that $k(1128nm) = 1.793cm^{-1}$ as suggested in (Cachorro et al., 2022). The reported value of $k(1128nm)$ has been calculated using a triangular slit function of 7 nm of Full Width at Half Maximum (FWHM) similar to the specification of the 1128 nm EnMAP band. We also assumed that the aerosol optical thickness at 550 nm is equal to 0.085 and the aerosol Angström exponent is equal to 1.2, which corresponds to average values of these parameters for the area studied (Tomasi et al., 2015). Taking into account that the retrievals are performed in the near infrared, one does not expect any significant retrieval errors due to assumptions related to light scattering by aerosol particles suspended in clean polar atmosphere.

As expected, the TCWV increases towards the lower ice-covered part of the melting glacier (lower part of Fig. 2), whereas the values of the total column of water vapor are slightly smaller over snow-covered area positioned at a high elevation (0.8–1 km). The same conclusions can be

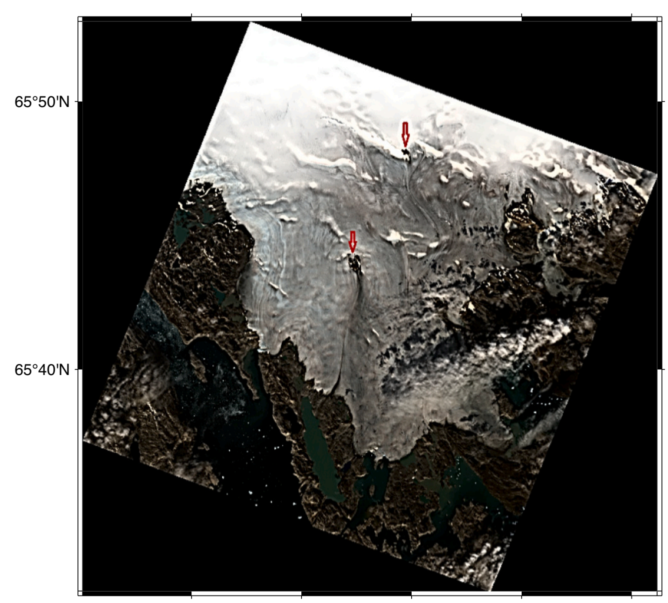

Fig. 1. The EnMAP true color RGB of the study area in South-Eastern Greenland derived from at - sensor radiance (September 6, 2025, 14:51:13 UTC). The arrows indicate the bare rocks inside glacier and origins of dirty rivers propagating downwards.

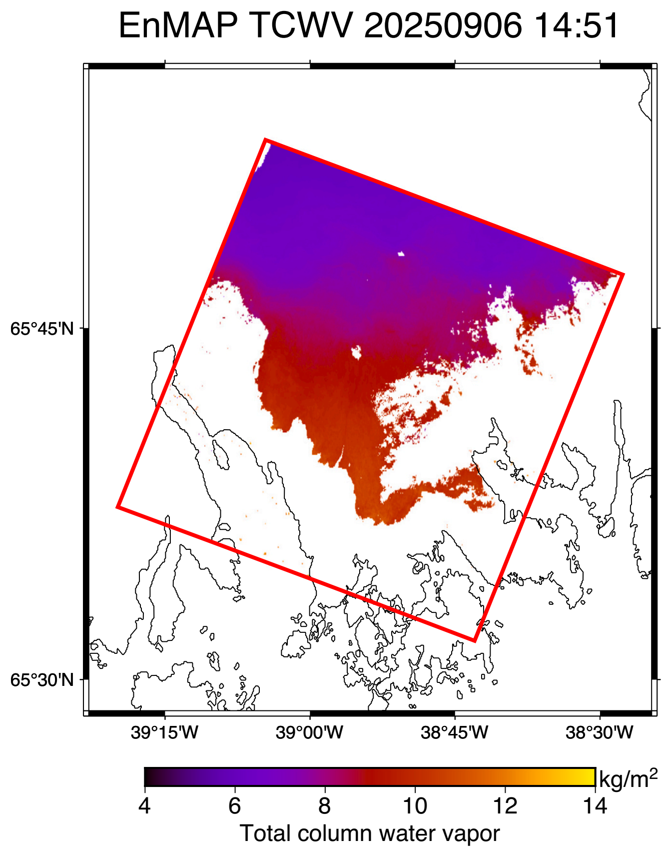

Fig. 2. The retrieved TCWV (kg/m^2) over glacier using EnMAP measurements.

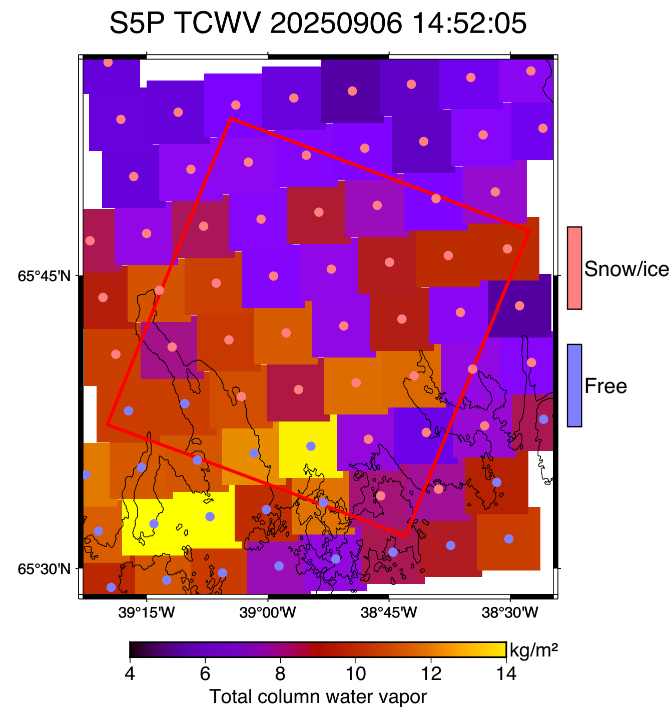

Fig. 3. The S5P total water vapor column (kg/m^2) retrievals performed at 14:52:05 UTC. The black line is the coastline. The red box shows the location of the EnMAP granule analyzed. The color dots show free of snow and ice ground pixels (blue color) and snow/ice covered ground pixels (red color). The difference in time of selected measurements performed by EnMAP and S5P is less than 1 min. (For interpretation of the references to color in this figure legend, the reader is referred to the web version of this article.)

reached analysing the retrievals performed by the ESA S5P instrument shown in Fig. 3, including also retrievals over bare land and ocean. The measurements from both platforms have been performed almost simultaneously (less than 1 min difference) and at the same location. One concludes comparing Figs. 2 and 3 that both EnMAP and S5P algorithms separate pixels covered by snow and ice in a coherent way. The S5P TCWV retrievals have been performed using the measurements in the weak water absorption band located at 435-455 nm as discussed in (Chan et al., 2022). The S5P algorithm consists of two parts: a Differential Optical Absorption Spectroscopy (DOAS) fit for calculating the slant column density of water vapor and conversion to vertical columns using box air mass factors calculated iteratively with the radiative transfer model. In the case of partial cloud cover, the algorithm uses an intensity-weighted cloud fraction to scale the clear and cloudy air mass factors, while *a priori* water vapor profile is replaced below the cloud deck and added to the water vapor column above cloud to compute the TCWV value.

The S5P performs measurements with much coarser spatial resolution (3.5 km × 5.5 km). Therefore, all EnMAP retrievals inside one S5P pixel have been averaged following the collocation procedure described in (Kokhanovsky et al., 2007). We have derived the average TCWV and also the coefficient of variance $c = s/N$ for TCWV inside S5P pixels. Here s is the standard deviation and N the number of EnMAP pixels inside the S5P ground scene. The comparison of the TCWV derived from EnMAP and S5P is shown in Fig. 4a as the function of latitude. The correlation plot is given in Fig. 4b, where the best quality S5P retrievals are located in the shaded area. The coefficient of variance and the absolute difference $d = TCWV_{S5P}$ - $TCWV_{ENMAP}$ are given in Fig. 5.

The difference in the retrieved TCWV decreases with latitude because for larger latitudes the underlying surface is more homogeneous (mostly snow). The value of S5P TCWV strongly fluctuates towards south, which is most probably related to the errors of the retrievals for inhomogeneous surfaces. This is due to the fact that S5P TCWV retrievals are performed under assumption of homogeneous ground pixels with a given albedo value, which is violated for inhomogeneous surfaces, and explains why the correlation coefficient r for datasets shown in Fig. 4b is not high ($r = 0.68$). The EnMAP TCWV fluctuations are at much lower level.

The average coefficient of variance of the retrieved TCWV inside one S5P pixel is just 4%, which confirms the suitability of the TCWV spatial resolution selected for the TCWV S5P product. The average values of TCWV derived for the whole 30kmx30km EnMAP granule from both instruments almost coincide (8.3 ± 1.5 kg/m^2 as derived from EnMAP and 8.4 ± 1.9 kg/m^2 as derived from S5P measurements). They are also close to the value TCWV = 8.8 kg/m^2 derived as a result of independent atmospheric correction of EnMAP data, which have been obtained in the framework of the differential absorption technique established in (Schläpfer et al., 1998) and provided for the whole EnMAP 30kmx30km granule in L1C EnMAP dataset (de Reyes et al., 2023). Taking into account the variability of the water vapor on the scale 30kmx30km as given in Fig. 2, we propose to provide TCWV for each 30 m EnMAP pixel in the official EnMAP L1C dataset instead of a single value for the whole granule as it is done in EnMAP L1C dataset right now.

4. Conclusion

In this work we compared the retrievals of TCWV performed using EnMAP with those derived from spatially and temporally collocated S5P measurements over a glacier. An excellent correspondence has been found with an average bias for the whole area equal to -0.25 kg/m^2 and RMSD 1.24 kg/m^2 The maximal bias equal to -5 kg/m^2 (see Fig. 5) was found at the boarders of the glacier with highly inhomogeneous surfaces. For most of S5P pixels, the absolute value of difference with EnMAP measurements was smaller than the nominal 2 kg/m^2 accuracy threshold (see Fig. 5). This is an excellent result taking into account that

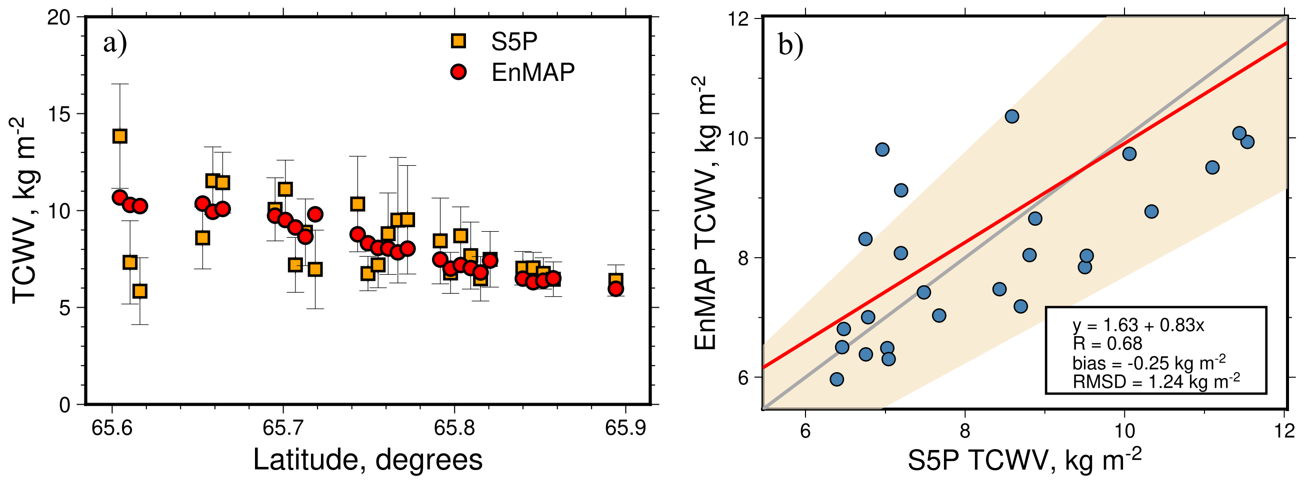

Fig. 4. (a) The dependence of the retrieved TCWV (kg/m^2), derived from EnMAP and S5P, on the latitude north of 65.5°. (b) Scatterplot of S5P and EnMAP TCWV with the empirical one standard deviation envelope as shaded area from the S5P TCWV per-pixel precision data.

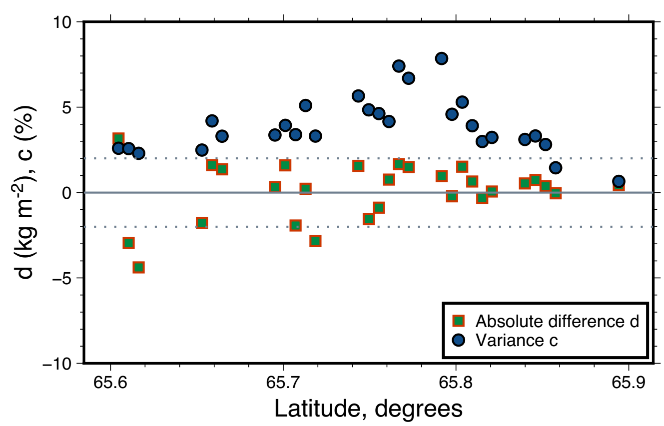

Fig. 5. The dependence of the absolute difference d (kg/m^2) and the coefficient of variance c on the latitude for collocated pixels.

the errors of the water vapor retrievals using EnMAP in the framework of other available algorithms is in the range 1.7–8.8 kg/m^2 as established by the comparison with ground measurements (Cremer et al., 2025). Unfortunately there was no coincident ground measurements of TCWV at the location studied. This is the limitation of the current work and an important avenue of future research.

However, taking into account that S5P TCWV values are close to those derived using ground measurements as it has been found in (Garane et al., 2023), we may confirm that the new EnMAP TCWV algorithm is capable to perform accurate measurements of water vapor total column with a high spatial resolution. We also see that EnMAP TCWV generally increases towards ocean and has the small variance within TCWV values, which supports the proposed single wavelength TCWV retrieval algorithm. This paper can be considered as an extension of the algorithm validation started in (Kokhanovsky et al., 2023a) for very dry conditions of Antarctica with underlying dry snow surface composed of small ice crystals.

It has been assumed in the framework of the EnMAP retrieval algorithm that both snow and glacier ice are semi-infinite weakly absorbing light scattering media, which is a good approximation for the reality (especially for the upper portion of the glacier). The EnMAP retrievals of TCWV are based on measurements in the near - infrared, where the influence of atmospheric light scattering characteristics and unknown light absorbing impurities in snow is reduced as compared to the visible region of the electromagnetic spectrum.

We also studied the intra-pixel variability of TCWV inside S5P pixels. It has been found that the coefficient of variance is less than 4% on average. This confirms the suitability of the S5P spatial resolution for the study of the water vapor spatial distribution for the case studied. Nevertheless, there is a large difference in the application of the two sensors for the TCWV retrievals, when it comes to surfaces with local sources of water vapor, where retrievals are only possible with EnMAP.

CRediT authorship contribution statement

Alexander Kokhanovsky: Writing – review & editing, Writing – original draft, Visualization, Validation, Software, Resources, Project administration, Methodology, Investigation, Funding acquisition, Formal analysis, Data curation, Conceptualization. **Luca Lelli:** Writing – review & editing, Writing – original draft, Visualization, Validation, Software, Methodology, Investigation, Formal analysis, Data curation, Conceptualization. **Karl Segl:** Writing – review & editing, Writing – original draft, Visualization, Validation, Supervision, Software, Resources, Project administration, Methodology, Investigation, Funding acquisition, Formal analysis, Data curation, Conceptualization. **Jörg Bendix:** Writing – review & editing, Writing – original draft, Supervision, Resources, Project administration, Methodology, Investigation, Funding acquisition, Conceptualization.

Declaration of competing interest

The authors declare that they have no known competing financial interests or personal relationships that could have appeared to influence the work reported in this paper.

Acknowledgements

This research was supported by the German Science Foundation (DFG) Deutsche Forschungsgemeinschaft (grant no. KO 3671/8-1/AOBJ 712291), the EnMAP science program (German Space Agency) with resources from the German Federal Ministry of Economic Affairs and Climate Action (grant no. 50EE1923). The TROPOMI TCWV processor was developed by DLR with national funding and deployed in the S5P Product Algorithm Laboratory (S5P-PAL) project and its data can be downloaded at https://data-portal.s5p-pal.com/products/tcwv.html. The S5P-PAL is funded by the EU and ESA and provides a platform for atmospheric processors based on Copernicus Sentinel-5P data. The authors are grateful to A. Smirnov for the discussions related to atmospheric correction procedures in polar atmospheres, B. Vandecrux for the ground observations of a studied glacier collocated with satellite measurements, and N. Bohn for important comments related to the first version of the paper. The authors also thank anonymous reviewers for careful reading of the paper and useful remarks, which led to the considerable improvement of the initial manuscript.

Appendix A. Appendix

In this Appendix we propose several EnMAP spectral indices to distinguish clouds and various underlying surfaces relevant to this study. They are

- snow;
- glacier ice;
- water;
- rocks.

The selection of pixels suitable for the processing using our TCWV retrieval technique is performed in the following way. First of all we reject all pixels with reflectance R(1026 nm) < 0.08 labelling them as water. Other surfaces listed above and also clouds have larger reflectances at this channel. Secondly, we check the reflectivity R(418 nm). We assume that cases with R(418 nm) < 0.3 correspond to rocks. The cloud screening is based on the analysis of spectral indices

$$\sigma_1 = \frac{R(1379nm)}{R(2199nm)}, \sigma_2 = \frac{R(1235nm)}{R(418nm)}. \quad (A.1)$$

We assume clouds, if $\sigma_1 \leq 0.03$ or $\sigma_2 \geq 0.3$ and R(418 nm) ≥ 0.3 simultaneously. The condition for σ_2 has roots in the fact that clouds near infrared reflectance is much closer to the visible light reflectance due to much smaller size of light scattering particles in clouds as compared to those in snow and glacier ice. The glacier ice corresponds to the case R(418 nm) ≥ 0.3 and $\sigma_2 < 0.15$. Otherwise, the surface is classified as snow. An example of the pixel identification routine for the case of EnMAP measurements shown in Fig. 1 is given in Fig. A1. Comparing both figures, one can see that the simple and fast pixel identification algorithm proposed above produces results suitable for the usage in the automatic TCWV retrieval procedure developed by us. It is important to note that the fixed thresholds given above may depend on the satellite viewing angle. However, EnMAP measurements are performed in the nadir direction. This fact together with low variation of the solar zenith angle during the observation time in polar regions makes it possible to consider the fixed thresholds given above for other locations in Greenland as far as EnMAP observations are of concern.

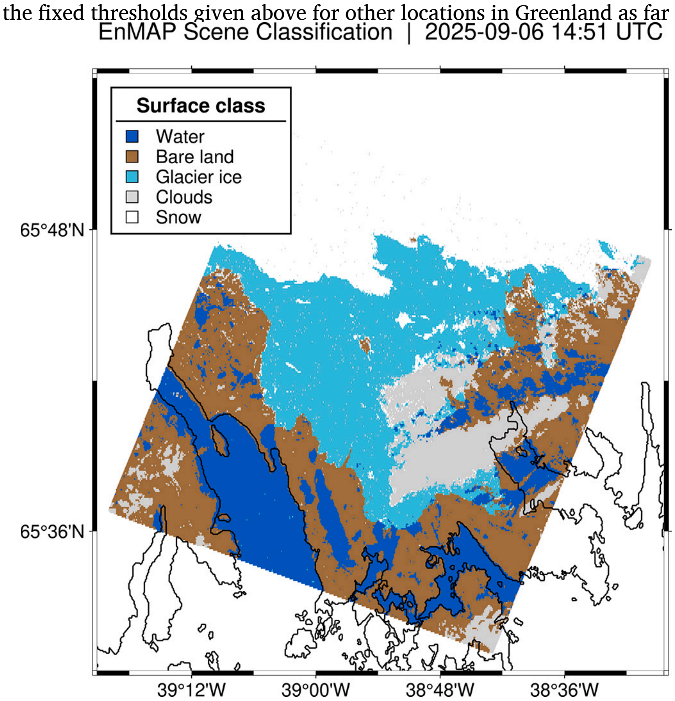

Fig. A1. The illustration of the performance of the pixel identification algorithm (0- water, 1-bare land, 2-glacier ice, 3-clouds, 4-snow). The respective EnMAP true color browse image is shown in Fig. 1.

Data availability

Data will be made available on request.

References

Cachorro, V.E., Antuña-Sanchez, J.C., de Frutos, A.M., 2022. SSolar-GOA v1.0: a simple, fast, and accurate spectral solar radiative transfer for clear skies. Geosci. Model Dev. 15, 1689–1712.

Chabrillat, S., Foerster, S., Segl, K., et al., 2024. The EnMAP spaceborne imaging spectroscopy mission: initial scientific results two years after launch. Remote Sens. Environ. 315, 114379. https://doi.org/10.1016/j.rse.2024.114379.

Chan, K.I., Xu, J., Slijkhuis, S., Valks, P., Loyola, D., 2022. TROPOspheric monitoring instrument observations of total column water vapour: algorithm and validation. Sci. Total Environ. 821, 153232. https://doi.org/10.1016/j.scitotenv.2022.153232, 2022.

Cremer, N., Alonso, K., Doxani, G., et al., 2025. Atmospheric correction inter-comparison eXercise, ACIX-III land: an assessment of atmospheric correction processors for EnMAP and PRISMA over land. Remote Sens. 17, 3790.

de los Reyes, R., Langheinrich, B., Bachmann, M., 2023. Level 2A Processor (Atmospheric Correction Over Land) ATBD. In: https://www.enmap.org/data/doc/EN-PCV

-TN-6007_Level_2A_Processor_Atmospheric_Correction_Land.pdf (last access: 12.12.2025).
Garane, K., Chan, K.K., Koukouli, M.-E., Loyola, D., Balis, D., 2023. TROPOMI/S5P total column water vapor validation against AERONET ground – based measurements. Atmos. Meas. Tech. 16, 57–74.
Green, A.E., Wagner, J.C., Mann, A., 1988. Analytic spectral functions for atmospheric transmittance calculations. Appl. Opt. 27, 2266–2272.
Guanter, L., Kaufmann, H., Segl, K., et al., 2015. The EnMAP spaceborne imaging spectroscopy mission for earth observation. Remote Sens. 7 (7), 8830–8857. https://doi.org/10.3390/rs70708830.
Hersbach, H., Bell, B., Berrisford, P., et al., 2020. The ERA5 global reanalysis. Q. J. R. Meteorol. Soc. 146, 1999–2029. https://doi.org/10.1002/qj.3803.
Kokhanovsky, A., 2022. The approximate analytical solution for the top-of-atmosphere spectral reflectance of atmosphere—underlying snow system over Antarctica. Remote Sens. 14, 4778.
Kokhanovsky, A., Brell, M., Segl, K., Chabrillat, S., 2024. SNOWTRAN: a fast radiative transfer model for polar hyperspectral remote sensing applications. Remote Sens. 16, 334. https://doi.org/10.3390/rs16020334.
Kokhanovsky, A., Chevrollier, L.-A., Wehrlé, A., Segl, K., Chabrillat, S., 2026. A simple analytical model for the reflection function of flat glacier ice surfaces and its application for optical remote sensing of glaciers. J. Quant. Spectrosc. Radiat. Transf. 351, 109717. ISSN 0022-4073. https://doi.org/10.1016/j.jqsrt.2025.109717.
Kokhanovsky, A., Vandecrux, B., Wehrlé, A., A., Danne, O., Brockmann, C., Box, J.E., 2023b. An improved retrieval of snow and ice properties using spaceborne OLCI/S-3 spectral reflectance measurements: updated atmospheric correction and snow impurity load estimation. Remote Sens. 15, 77.
Kokhanovsky, A.A., Brell, M., Segl, K., Bianchini, G., Lanconelli, C., et al., 2023a. First retrievals of surface and atmospheric properties using EnMAP measurements over Antarctica. Remote Sens. 15 (12), 3042. https://doi.org/10.3390/rs15123042.
Kokhanovsky, A.A., Nauss, T., Schreier, M., von Hoyningen-Huene, W., Burrows, J.P., 2007. The intercomparison of cloud parameters derived using multiple satellite instruments. IEEE Trans. Geosci. Remote Sens. 45 (1), 195–200. https://doi.org/10.1109/TGRS.2006.885019.
Pierluissi, J.H., Tsai, C.-M., 1986. Molecular transmission band model for oxygen in the visible. Appl. Opt. 25, 2458–2460.
Platt, U., Stutz, J., 2026. Differential Optical Absorption Spectroscopy. Springer, Berlin.
Schläpfer, D., Borel, C.C., Keller, J., Itten, K.I., 1998. Atmospheric pre-corrected differential absorption technique to retrieve columnar water vapor. Remote Sens. Environ. 65, 353–366.
Tomasi, C., Kokhanovsky, A.A., Lupi, A., et al., 2015. Aerosol remote sensing in polar regions. Earth Sci. Rev. 140, 108–157. https://doi.org/10.1016/j.earscirev.2014.11.001.